Motorcycle Modelling and Trajectory Controlling

Miguel Zambujo Orvalho
miguel.orvalho@tecnico.ulisboa.pt

Instituto Superior Técnico, Universidade de Lisboa, Portugal

October 2021

Abstract

The knowledge of the dynamic behavior of a motorcycle, allows its development and performance improvement, mainly at the level of competition. In the present work, the dynamic behaviour of a motorcycle is discussed, referring to limit conditions in different scenarios, and some dynamic aspects related to the steering movement are highlighted. The formulation necessary for the construction of a multibody model of a motorcycle is presented, where a kinematic "driver" for steering control is also implemented. The main external forces involved in a road vehicle are discussed and it is approached some of the most used tire models in describing the forces involved in the contact between the tire and the road. The detection of this contact is also described. The expressions of the kinematic quantities necessary for the implementation of the tire model *Pajecka Magic Formula* are discriminated, where its implementation is compared with the literature. The multibody model is based on the TLM03e electric prototype developed by the TLMoto team in IST. The motorcycle model is tested in the simple straight-line scenario. The control of the motorcycle is presented through the implementation of an LQR controller. A reduced model is suggested, for controlling the motorcycle in different scenarios.
Keywords: Multibody Dynamics, Motorcycle Dynamics, Pacejka Magic Formula, Motorcycle Control, Racing Motorcycle

1. Introduction

In the framework of motorcycle dynamics, control can be used to simulate a perfect rider in a track, in order to reach a performance goal or to reveal system limitations. It is also applicable on situations of overcome instant human control, such as in driverless condition, or to support the rider in specify trajectories.

Vehicle dynamics play an important role in the engineering world as it is used daily for human mobility and the transportation of resources. With regard to motorcycles, they are increasingly used in the choice of short courses. Therefore, an understanding of the fundamental behaviour of motorcycles is required to reveal the mechanisms for control, and to highlight the conditions of instabilities that dangerously affect the rider's control capabilities. One of the aspects of the two-wheel system is that it is an unstable system by nature, at low speeds. It has a range of velocities in which it is self-stable, where the necessary forces in the front wheel are developed to self-stabilize but, for higher velocities becomes unstable again [3]. Another aspect of two-wheeled vehicles is the non-intuitive movement of the steering to describe a curve [3, 19].

A typical approach to study a mechanical system is to define it as a multibody system. A multibody system is composed by bodies or links, which the motion between each can be constrained by internal and external forces. The bodies are connected by kinematic joints, formulated by kinematic constraints equations [12]. Among the various possibilities of external forces that can act on a system, in dynamic road vehicles, greater importance is given to the tire's contact with the ground. Many authors present different options for contact models [18, 5], but in order to portray the contact between tire and road, these stand out [6, 7, 8][13]. Many commercial software are used to preform dynamic analysis, but the program MUBODyn-Matlab, developed and created at IST, is the one used on this work. Since the contact between the tires and the ground is extremely important in dynamic vehicles, the attempt to reproduce it has been a subject of study over the years. An analytical tire model was proposed by [6, 7, 8], but more attention was payed to the semi-empirical tire model developed by [13], where a standard formula is used to calculate almost all forces developed in contact. Also in [13], a specific tire model for motorcycles was developed in order to meet the wide ranges of roll angle described by them.

Also associated with external factors, such as wind or the condition of the ground, motorcycles are known to destabilize in two ways - weave and wobble instability effects [14]. One of the ways to study the appearance of these effects is to know the behaviour of the motorcycle through a control system. For this work the implementation of a virtual driver is the focus of the control system. A control methodology is presented in [10] for a car with four-wheel steering and application of traction and braking torques to each one of them. The strategy is later implemented in Matlab by [1] using a bicycle model. A state-feedback control such as linear quadratic control, is commonly used to control a motorcycle. In [11], both feedback and feedforward control are used to control a motorcycle by steering, by applying a torque on it. There is no such thing as equations that exactly describe the dynamic behaviour of a motorcycle. Therefore, one of the measures that can dictate a good control system, is the choice of state variables and the simplified equations that describe the motorcycle dynamics. In [16] can be found the derivation of simplified equations of motion, where is later applied to motorcycle by [11]. Describing a trajectory over a reference line is one of the great challenges faced by many authors on motorcycle control. A road preview is one of the strategies used, as it is similar to the way a human drives a vehicle [17].

This paper is structured as follows. In section 2, an overview regarding the dynamics of the motorcycle is presented. For section 3, the multibody dynamics used to simulate the motorcycle dynamics is formulated, where a formulation of a steering driver is included. The section 4 concentrates on the implementation of the tire model and the contact detection is described with detail. In section 5, the motorcycle model is formulated and it is presented the first scenario in a straight line with an unassisted motorcycle. In section 6, the reduced model is defined along with the implementation of the controller and the motorcycle is finally tested with control in some scenarios, where it is increased the difficult of control. Lastly, in section 7, conclusions are presented together with recommendations for future work.

2. Overview of Motorcycle Dynamics

Motorcycles are an unstable vehicle by nature, due to the fact that they must balance on two small contact areas with the ground. The geometric parameters of the vehicle have a great importance in motorcycle dynamics and stability, since they define the purpose of the motorcycle. Reference works, such as those by Cossalter [3] and Foale [19] present a detailed description of motorcycle dynamics, the influence of its geometry and of the many characteristic phenomenons associated to acceleration, braking, cornering and other dynamic characteristics and responses.

2.1. Motorcycle Geometry

Geometric parameters are used to characterize a motorcycle. Different sets of parameters lead to different dynamic behaviour, being those of the sport, off-road or touring motorcycles distinct from each other. Figure 1 shows some of the parameters more important to characterize a motorcycle.

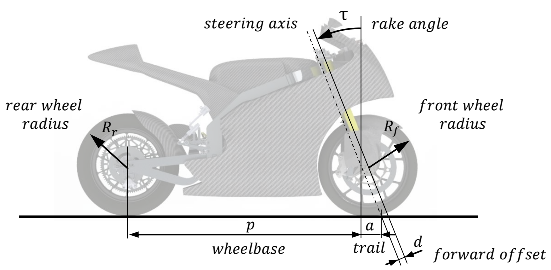

Figure 1: Geometric parameters that characterize a motorcycle.

Note that more stability means less maneuverability, being important to maintain an equilibrium between both in accordance to the purpose of the motorcycle. An increase of the parameters p, τ and a, means more stability for the motorcycle.

2.2. Rectilinear Motion

A rectilinear motion of a motorcycle can be seen as pure accelerating or braking scenarios. However, some limits for both cases are assumed considering steady state motion for simplicity. Figure 2 shows the angular motion around the common inertia axes, with origin on the center of mass of the motorcycle frame. This reference frame is used to describe motorcycle dynamics in general and the particular aspects of the virtual rider dynamics of this work, in particular.

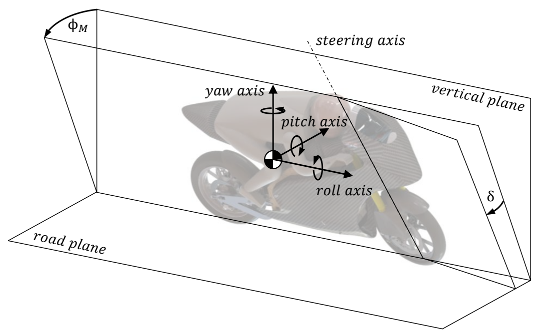

Figure 2: Definition of the inertia axis for the motorcycle dynamics. ϕ_M is the roll angle and δ the steering angle.

The moments of inertia around the roll, pitch and yaw axis are some of the most relevant mass associated parameters for the motorcycle dynamics. The roll moment of inertia influences the "resistance" of the motorcycle to the roll motion. Maintaining the center of gravity position, high values of roll moment of inertia slow down the entry and exit in a curve. Yaw moment of inertia influences the maneuverability as high values of yaw moment reduce the handling ability of the motorcycle. The pitch inertia, together with the wheelbase, have a strong influence on the motorcycle longitudinal dynamics, due to its ability to use both rear and front tires for braking/traction.

2.3. Cornering

In a cornering scenario, a motorcycle has to lean to compensate the centrifugal forces due to the curving of the motorcycle. Considering steady state motion and neglecting some of the gyroscopic effects, a motorcycle in cornering can be understood in plane, simply by the force equilibrium between the centrifugal and gravity forces as shown on the figure 3, i.e., the direction of the resultant must intersect the line on the road between the two contact patches of the tire.

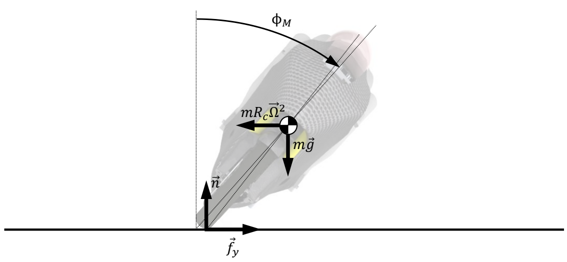

Figure 3: Motorcycle under Cornering (adapted from [3]).

It is interesting to consider the case of a motorcycle entering in a curve, considering gyroscopic effects, which relates to the steering position of the motorcycle. Say that the motorcycle is to turn to a right curve. Contrary to the intuition, the handlebars are first turned to the left producing the effect of leaning the motorcycle to the right, due to the lateral force on the front wheel and gyroscopic moments. While entering the turn, the handlebars are slowly turned to the right to ensure the proper roll of the motorcycle in order to follow the required trajectory, i.e, to perform the right side curving.

3. Multibody Dynamics Formulation

Assuming that the flexibility of each one of the system components can be neglected, the analysis of a rigid body system allows calculating the forces acting on it. The procedure to identify the rigid bodies and to define the constraints between them is overviewed in order to describe the modeling facilities provided by the methodology used here. The forces applied on the motorcycle are also discussed, with particular interest on the contact forces of the tires.

3.1. Coordinates of the Multibody System

A rigid body uses six independent coordinates to represent its kinematics, being three for translation and three for rotation. Translation and rotation of a rigid body i is given by the position of its fixed frame (ξ, η, ζ) and the rotation of its axis relative to the global frame (X, Y, Z). Using Cartesian coordinates to define the position $\mathbf{r}_i = [x, y, z]^T$ and Euler parameters for rotation $\mathbf{p}_i = [e_0, e_1, e_2, e_3]^T$, in which one of the parameters is dependent [12]. The vector that defines the rigid body i position and orientation is $\mathbf{q}_i^* = [r_i^T, p_i^T]^T$.

The position, in global coordinates, of a point P belonging to the rigid body i, is described by vector $\mathbf{r}_i$ written as:

$$\mathbf{r}_i^P = \mathbf{r}_i + \mathbf{s}_i^P = \mathbf{r}_i + \mathbf{A}_i \mathbf{s}_i'^P \tag{1}$$

where $\mathbf{A}_i$ is the transformation matrix from body i coordinates to the inertia frame coordinates.

3.2. Kinematic Constraints

The kinematic constraints, representing the restrictions between the relative motion of the rigid bodies, are described by algebraic equations. These constraints are used to represent mechanical joints. By choosing the suitable kinematic joints, the behavior of a system of linked bodies can be modeled to satisfy the correct system mobility. In the case of application of this work, the motorcycle multibody model is described by two types of joints: revolute and translational joints [12].

Revolute joints allows for a single rotation of two bodies around a common axis, thus preventing any other relative motion. This means that two parallel vectors on each body remain parallel after they move, always sharing a common point. Revolute joint has a single degree of freedom. Thus requiring five algebraic equations to represent the kinematic constraints.

Translational joints allow for the translation of two bodies through a common axis while preventing any relative rotation. The translational joint is defined by enforcing the orthogonality between different vectors. This joint has also a single degree of freedom, being in this case a relative translation. Thus requiring five algebraic equations to represent the kinematic constraints.

For the purpose of motorcycle control, there is the need to define one more constraint. To control the steering with the handlebars, this constraint is defined as a driver constraint in a revolute joint. Two vectors are given, $\mathbf{v}_i$ and $\mathbf{v}_j$, to regulate the angle δ between the two bodies in a revolute joint. The vector $\mathbf{v}_i$ is perpendicular to the vector $\mathbf{s}_i$, and $\mathbf{v}_j$ is perpendicular to $\mathbf{s}_j$. Vector $\mathbf{v}_j$ is also parallel to

$\mathbf{v}_i$ when the two bodies are aligned, enforcing that the steering angle δ is null. To manage the angle δ, a cross product is used to define the constraint equation.

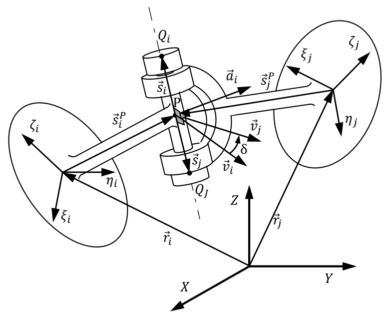

Figure 4: Driver for steering.

The driver is defined by a single algebraic constraint, which is the steering angle δ, related to the orientation of bodies i and j.

3.3. Equation of Motion

For any multi-body system, integrated with kinematic constraints and rigid bodies, the governing equilibrium equations are expressed as:

$$\begin{bmatrix} \mathbf{M} & \mathbf{\Phi}_q^T \\ \mathbf{\Phi}_q & 0 \end{bmatrix} \begin{Bmatrix} \ddot{\mathbf{q}} \\ \boldsymbol{\lambda} \end{Bmatrix} = \begin{Bmatrix} \mathbf{g} \\ \boldsymbol{\gamma} - 2\alpha\dot{\mathbf{\Phi}} - \beta^2\mathbf{\Phi} \end{Bmatrix} \tag{2}$$

Here, $\mathbf{M}$ is the mass matrix, $\mathbf{\Phi}_q$ is the Jacobian matrix related to the kinematic constraints, $\ddot{\mathbf{q}}$ is the accelerations vector of the system, $\boldsymbol{\lambda}$ is the vector of Lagrange multipliers associated to the joints reaction forces, $\mathbf{g}$ is the force vector, $\boldsymbol{\gamma}$ is the right-hand side of the acceleration constraints equations, $\dot{\mathbf{\Phi}}$ is the first time derivative of the kinematic constraints $\mathbf{\Phi}$ and α and β are parameters associated with the Baumgarte Stabilization [2].

For a rigid body i, provided that the body fixed frame $(\xi, \eta, \zeta)_i$ is fixed to its center of mass and that the axis are coincident with its principal inertia axis, the matrix $\mathbf{M}_i$ is diagonal and filled with the mass and principal inertial moments of the body,

To solve the system of equations in 2, it is necessary to set initial conditions. The parameter t_0 is the initial instant of time to start the simulation, $\mathbf{q}^*_{t_0} = \mathbf{q}^*_i$ the initial vector of position and orientation, and $\dot{\mathbf{q}}^*_{t_0} = \dot{\mathbf{q}}^*_i$ the initial velocity vector.

In order to understand and computationally implement the algorithm of the multibody equation of motion, a flowchart is shown in the Figure 5. The Baumgarte parameters are set to $\alpha = 5$ and $\beta = 5$, proving to be good values as as suggested in [2].

3.4. Applied Forces to the Multibody System

The suspension has an important role in vehicle dynamics as the handling characteristics of the motorcycle strongly depend on them. The most important components of the suspension systems are translational spring-damper components. The force developed by the suspension element is computed through the sum of the spring and damper forces, f^k and f^c respectively. The force felt in body i is represented as:

$$\mathbf{f}_i^{kc} = \left(f_i^k + f_i^c\right)\mathbf{u} \tag{3}$$

while the force on body j is the opposite of that on the other body, since body i and j are a reaction action pair, the forces felt in each body are equal in magnitude, but with different signal. The unit vector $\mathbf{u}$ is aligned with the attached points of each body.

Every type of systems are integrated on a medium, and the interaction between the system and the medium influences the system behaviour, beyond the internal forces developed inside the system. This interaction can be seen in a multibody system perspective, as external forces applied to it. For road vehicles, the main interaction is usually with the road, that is relatively rigid. This interaction is commonly described by contact forces models [18, 5]. Contact between two bodies is often characterized by the normal and friction forces developed in each sliding body surface, and the stiffness and damping of the body that is treated as dissipative energy.

In this work, the multibody system is a motorcycle and the contact is made between the road and the pneumatic tires, being the generic forces developed represented in Figure 6.

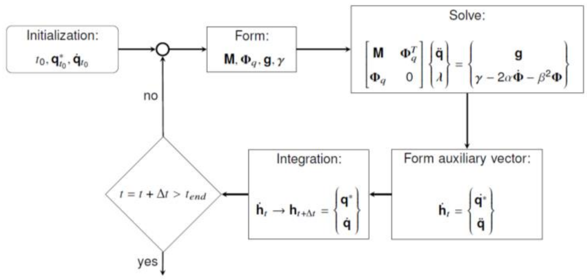

Figure 5: Flowchart of multibody dynamics program.

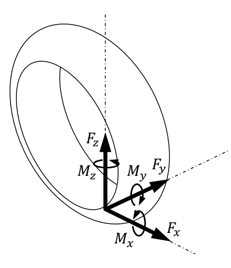

Figure 6: Forces and moments on pneumatic tire due to its interaction with the road.

Among the model options, two models are considered for the implementation: an analytical model developed by Gim and Nikravesh [6, 7, 8] and a semi-empirical one developed by Pacejka [13]. Among these, the Pacejka tire model is the mostly used by the industry and being its parameters available for the application foreseen here and, therefore, it is selected to be implemented in this work.

4. Tire Forces Implementation

The tire force evaluation requires that contact is first detected and, if it exists, that the proper kinematic quantities of the wheel and road are defined. Afterwards, the tire force model is used to evaluate the tire forces and moments. In this section, the tire model known as *Pacejka Magic Formula* developed in [13] is presented with the assumptions purposed by Sharp [15]. The implementation of the *Pacejka Magic Formula* tire model is presented and the demonstration of its performance compared with of the [15]. Finally, the tire contact forces are applied to the wheel body in which the tire is mounted.

4.1. Contact Detection

The contact detection is the first step on tire forces calculation. The contact search consists in identifying the contact patch and evaluating an indentation between the tire geometry and road. The unevenness of the ground is well described by a triangular mesh. Each triangle is represented by three nodes numbered counterclockwise with respect to the normal of the triangle surface $\mathbf{u}_n$.

For every time step in contact detection algorithm, two main parts are identified. First it is assumed a flat horizontal road, and after the search for a triangular contact patch, all the quantities needed for the tire model are computed if there is penetration of the tire with the road. Second, if the triangular contact patch found is not horizontal, the quantities are computed again for the new triangular contact path. Figure 7 reveals all the points, referential systems and quantities needed for better understanding.

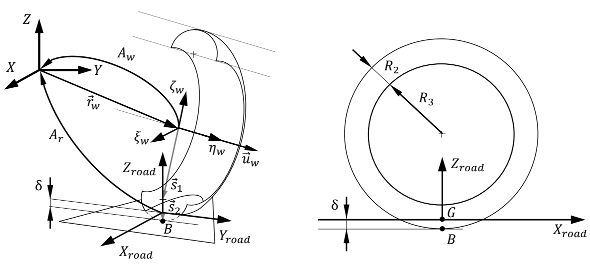

Figure 7: Axis system necessary and important points in contact search.

Figure 7 shows that the tire can be approximated to a toroidal body, with a revolution R_3, of a crown with radius R_2. Point G is the contact point with the road and B the point below, belonging to the crown surface. On the limit of the contact, B and G are the same. In order to search for a triangular contact patch, the position of point B is firstly defined assuming a flat horizontal road. The matrix $\mathbf{A}_r = \begin{bmatrix}\mathbf{u}_{xr} & \mathbf{u}_{yr} & \mathbf{u}_{zr}\end{bmatrix}$, represents the transformation matrix of the road coordinate system $(XYZ)_{road}$ to the global coordinate system (XYZ).

If the possible triangular contact path found is horizontal, $\mathbf{u}_n = \begin{bmatrix}0 & 0 & 1\end{bmatrix}'$, the penetration δ between the tire and the contact patch is evaluated by performing:

$$\delta = z^G - z^B \tag{4}$$

The quantities z^G and z^B are the z coordinates of point G and B, respectively. The quantity z^G is obtained from the expression which defines a plan as:

$$z^G = a + bx^B + cy^B \tag{5}$$

where a, b and c are the plan coefficients. Note that $x^G = x^B$ and $y^G = y^B$, since the triangular contact path found is horizontal. There is penetration between the tire and the road if $\delta > 0$, otherwise the search is initiated for the other tire and then advance for the next time step. The penetration δ, the position of the contact point $\mathbf{r}^G = \begin{bmatrix}x^G & y^G & z^G\end{bmatrix}'$ and the transformation matrix $\mathbf{A}_r$ are now defined for the case of having a horizontal contact patch.

To evaluate the penetration δ for the case of a non-horizontal contact patch, the equation 6 is used, where the coordinate z of the normal vector $\mathbf{u}_n$ of the contact patch is multiplied by the equation 4, following the expression:

$$\delta = \mathbf{u}_{n(z)}(z^G - z^B) \tag{6}$$

The contact is again verified if the rigid body wheel penetrates the road with $\delta > 0$, as illustrated in Figure 7. In order to compute the position of the contact point $\mathbf{r}^G$, equation 7 is given as:

$$\mathbf{r}^G = \mathbf{r}^B + \delta\mathbf{u}_n \tag{7}$$

For the case of the non-horizontal triangular contact patch, are defined the value of the penetration δ, the position of the contact point $\mathbf{r}^G$ and the transformation matrix $\mathbf{A}_r$.

4.2. Kinematic Quantities for Pacejka Magic Formula

The computation of the kinematic quantities to evaluate the forces acted on the tire, are common to some model, as [6, 7, 8] and [13]. Therefore, Figure 8 shows the important angles on tire dynamics used to compute the necessary kinematic quantities.

In order to calculate the slip quantities, it is important to understand how Pacejka defines the tire. The tire is seen as a thin disc, where the point C,

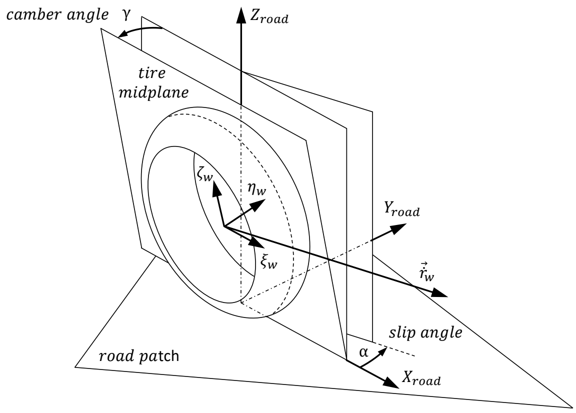

Figure 8: Important angles in tire dynamics.

shown in Figure 9, is the contact center point intersected by the disc and road. Point S, shown in Figure 9, is located at a distance from the wheel center equal to the effective radius r_e.

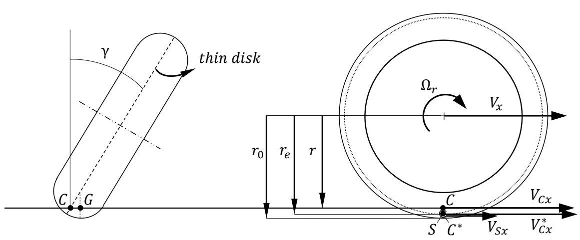

Figure 9: Location of point C, its velocity and slip velocity on point S (adapted from [13]).

For Pacejka, the slip quantities are evaluated around point C. To compute the position of point $\mathbf{s}_w^C$ with respect to the wheel center of mass, given by equation 8, is considered the position of the contact point G previously computed.

$$\mathbf{s}_w^C = \mathbf{s}_w^G + \mathbf{A}_r \left\{(R_2 - \delta)\tan(\gamma)\right\} \begin{Bmatrix} 0 \\ 1 \\ 0 \end{Bmatrix} \tag{8}$$

The position of the contact point $\mathbf{s}_w^G$ with respect to the wheel center of mass is given by $\mathbf{s}_w^G = \mathbf{r}^G - \mathbf{r}_w$ and γ is in fact the camber angle value expressed by equation 13. Longitudinal slip κ is given as the quotient between the longitudinal slip velocity V_{Sx} and longitudinal velocity V_{Cx}:

$$\kappa = -\frac{V_{Sx}}{max[|V_{Cx}|, \varepsilon_{Vx}]} \tag{9}$$

The longitudinal slip velocity, i.e., longitudinal velocity of point S, is given as $V_{Sx} = V_{Cx} - V_r$, where V_{Cx} is the longitudinal running velocity in point C and $V_r = \Omega_r r_e$ the rolling velocity, where Ω_r, seen in Figure 9, is the angular rolling velocity of the wheel. Covering all cases, V_{Cx} can be computed as follow, where $\boldsymbol{\omega}_w$ is the angular velocity of the wheel.

$$V_{Cx} = (\mathbf{A}_r^T \dot{\mathbf{r}}_w)^T \begin{Bmatrix} 1 \\ 0 \\ 0 \end{Bmatrix} - (\mathbf{A}_r^T \boldsymbol{\omega}_w)^T \begin{Bmatrix} 0 \\ 0 \\ 1 \end{Bmatrix} \left\|\mathbf{s}_w^C\right\| \sin(\gamma) \tag{10}$$

For a flat (or approximately flat) road, there is no angular variation between point S and wheel center. Cases where the velocity V_{cx} becomes null, it is replaced for a small quantity $\varepsilon_{Vx} = 10^-3$, also to calculate lateral slip ratio.

Lateral slip ratio α^* is defined as the tangent of the slip angle, computed as the quotient between lateral slip velocity V_{sy} and longitudinal velocity of point C. Using the modulus for V_{Cx}, backwards running is covered.

$$\alpha^* = \tan\alpha \cdot sgn(V_{Cx}) = \frac{V_{Sy}}{max[|V_{Cx}|, \varepsilon_{Vx}]} \tag{11}$$

V_{Sy} can be obtained as follows:

$$V_{Sy} = (\mathbf{A}_r^T \dot{\mathbf{r}}_w)^T \begin{Bmatrix} 0 \\ 1 \\ 0 \end{Bmatrix} - \left(\mathbf{A}_r^T \left(\begin{Bmatrix} 0 \\ 0 \\ -r_e \end{Bmatrix} \times \boldsymbol{\omega}_w\right)\right)^T \begin{Bmatrix} 0 \\ 1 \\ 0 \end{Bmatrix} \tag{12}$$

The value of camber angle, the resulting angle between the normal of the road and the thin disc, can be computed as:

$$\gamma = \frac{\pi}{2} - \arccos(\mathbf{u}_w^T \mathbf{A}_r \begin{Bmatrix} 0 \\ 0 \\ 1 \end{Bmatrix}) \tag{13}$$

Performed the computation of slip quantities - longitudinal slip κ, lateral slip α^* and the camber angle γ - the *Pacejka Magic Formula* will be used to ensure the forces developed on the tire.

4.3. Pacejka Magic Formula

If there is contact between tire and road, the *Pacejka Magic Formula* tire model can now be applied. The model used in this chapter is restricted for steady-state situation. The inputs necessary for the model are presented in the Table 1, as well as their outputs.

Table 1: Input variables necessary for the model and the outputs given.

Input	Output
longitudinal slip ratio, κ lateral slip ratio, α^* camber angle, γ F_z	F_x F_y M_x M_y M_z

The model is known by *Magic Formula*, because it is the used a single standard formula to compute different output values. Besides the input described in the table, the formula also needs non-dimensional parameters p, q, r and s, related to the tire used and some operation condition, and a set of scaling factors λ. The default values of λ will be considered.

Together with the kinematic quantities calculated in the previous section, the tire model also needs the vertical force F_z imposed on the tire as input. C_z is the radial stiffness coefficient of the tire and D_z its radial damping coefficient. The equation 14 of the vertical force presents a different form from the one used in [13].

$$F_z = C_z \delta - D_z \dot{\delta} \tag{14}$$

Proceeding to the computation of the forces vector $\mathbf{f} = \begin{bmatrix} F_x & F_y & F_z \end{bmatrix}'$ and moments vector $\mathbf{m} = \begin{bmatrix} M_x & M_y & M_z \end{bmatrix}'$, with the use of the *Pacejka Magic Fromula* expressions, the outputs of the tire model are all defined. To work with a symmetric tire model, the coefficients $S_{Hx\alpha} = S_{Hy\kappa} = S_{Vy\kappa}$ were set to zero [15], modifying some of the original tire parameters. With all the inputs expressed, the vector of forces $\mathbf{f}$ and moments $\mathbf{m}$ resultant on point C are transferred for the wheel body center of mass, in order to incorporate the $\mathbf{g}$ forces vector of the multibody system dynamics, as seen in Figure 5.

5. Multibody Model for the Motorcycle

All the multibody formulation made in Chapter 3 are used in order to characterize the rigid bodies, kinematic joints, suspension elements and tires of the motorcycle TLM03e. Finally, a simple scenario with the motorcycle model is presented.

5.1. Description of TLM03e

TLM03e is a racing track motorcycle developed by TLMoto team, a group of enthusiastic students for motorcycle engineering from Instituto Superior Técnico. The TLM03e is an electric motorcycle, developed with the aim of participating in an international competition called Motostudent.

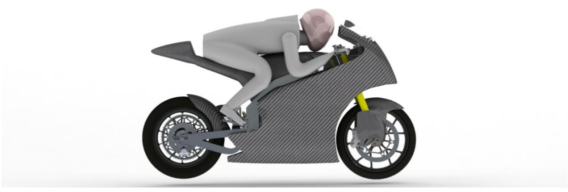

Figure 10: TLM03e CAD.

5.2. Multibody Model

To obtain the necessary values for the multibody model, a CAD software with the entire motorcycle is used to have a more accurate and faster acquisition of data. The data is taken considering the motorcycle hanging, in other words, no force applied by the suspension elements, and with the default mechanical setup. The motorcycle multibody model is composed of 6 rigid bodies where the rear suspension is not taking into account, since it has a very low weight. For dynamics purposes, body 3 is composed for the pilot, in a static position, and frame. The values of the mass properties and the principal moments of inertia were extracted for each rigid body. For each rigid body, the local coordinates system is positioned in its center of mass and aligned with the principal axis of inertia.

The kinematic joints are responsible for giving the bodies the desired motion between them. With all bodies defined, the kinematic constraints are formulated through the information of the constraint joints coordinates, taken in the fixed frame of the rigid body that is involved with the joints. For the whole model, this one is composed by 4 revolute joints and 1 translational joint.

The front suspension used on TLM03e is a fork telescopic, which is the most used, specially in this type of motorcycles. For the rear suspension, TLM03e is equipped with a monoshock attached to the frame and swingarm, being both suspensions composed by a spring and a damper.

The slick tires used on this motorcycle are: 90/580 R17 for the front tire and 120/600 R17 for the rear tire. The nomenclature to describe the tires refers to their size, where the first number is the width in millimeters, the second is the diameter of the tire in millimeters and the third is the radius of the rim in inches. Unfortunately, it is very difficult to find the tire properties database, on literature, for these tire sizes. By virtue of that, the tire parameters of 180/55 presented in section 4 were chosen to represent both tires' dynamic behaviour. Of course, the tire properties do not fit with the size, causing less accurate values on simulations. However, the tire parameters found on *Adams* software database are complete and consistent with the ISO system.

5.3. Scenario 1: Straight Line

To test the tire model along with the motorcycle model, a simple straightforward trajectory was attempted. In addition to post processed graphs resulting from the simulation, *SAGA* software was used to visualize graphically the motorcycle behaviour derived from the simulation. In this software all the dynamics information of each body is uploaded as well as the files with graphic information taken from a CAD software. Figure 11 shows the movement of the center of gravity of body 3 (Frame + Pilot) along with the trajectory prescribed. Although Figure 11 is representing the information of body 3, it also represents directly the entire motorcycle, since body 3 is its main body.

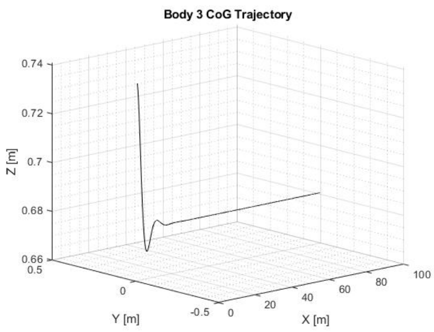

Figure 11: 3D trajectory of body 3.

6. Motorcycle Control

The control strategy used for the motorcycle is based on the work of [1]. In order to describe the motorcycle reduced model, the works of [11] and [4] were taking into account. It was decided to follow the structure of the simplified motorcycle equilibrium equations, for the motorcycle motion, presented in [11]. In the controller design, as demonstrated by [9], a LQR controller is used for motorcycle controlling purposes. The simplicity of the reduced model idea is also discussed as a way of control over a reference line.

6.1. Description of the Motorcycle Reduced Model

The variables to represent the state of the motorcycle must be defined before describing the simplified equations for motorcycle equilibrium. As seen in Chapter 2, motorcycle needs to lean to describe a curve. Thus, the lean angle ϕ needs to be added to the state vector. Using a bilinear control methodology, as shown by [1] and [9], the continuous-time state-space regulator form is defined by the next equation.

$$\dot{\mathbf{z}} = \mathbf{Cz} + \mathbf{Bu} + \mathbf{Nu} \tag{15}$$

A more reduced model can be used to control a motorcycle instead of those presented in [1] and [11]. A motorcycle could only use the steering angle δ and the lean angle ϕ information to maintain equilibrium, as referred and used by [4] and [9]. Therefore, the state vector can be reduced to:

$$\mathbf{z} = \begin{bmatrix} \delta & \phi & \dot{\delta} & \dot{\phi} \end{bmatrix}^T \tag{16}$$

To control the motorcycle under a constant velocity, the moments applied on the wheels are null. For that reason, the control vector is summarized as steering torque:

$$\mathbf{u} = \begin{bmatrix} M_h \end{bmatrix}^T \tag{17}$$

The motorcycle parameters used in the simplified equations for motorcycle equilibrium are consider with a fix value, since very small variations occur on the motorcycle geometry after its stabilization. It was consider the default values for i_a and λ founded in [11]. Through the simplified equations of motorcycle equilibrium derived, the matrices $\mathbf{C}$, $\mathbf{B}$ and $\mathbf{N}$ are achieved.

6.2. Design of the Controller

In this work, the controller takes the place of the rider with regard to the motorcycle stabilization. Using a controller based on the methodology proposed by [10] and used by [9] for control, the continuous-time state-space regulator is defined by equation 15.

Matrix $\mathbf{N} \in \Re^{n\times m}$ represents the sum of product of state variables by $\mathbf{N}_j$ matrices. In this case $o = 1$ with $z_1 = \phi$ and $\mathbf{N}_1 = \mathbf{N}_\phi$, however $\mathbf{N}_\phi$ is null.

Initial values for $\mathbf{z}$ are needed to initialize the controller model, $\mathbf{z}(0) = \mathbf{z}_0$. The state vector $\mathbf{z} \in \Re^n$ and the control vector $\mathbf{u} \in \Re^{n\times m}$, are related by the state-feedback law:

$$\mathbf{u} = -\mathbf{K}_{FB}(z)z \tag{18}$$

Where the optimal gain matrix $\mathbf{K}_{FB} \in \Re^{n\times m}$ is defined in a way that equation 18 minimizes the quadratic performance index J.

$$J = \frac{1}{2}\int_{t_0}^{t_\infty} (\mathbf{z}^T\mathbf{Qz} + \mathbf{u}^T\mathbf{Ru})dt \tag{19}$$

The symmetric weighting matrices $\mathbf{Q} \in \Re^{n\times m}$ and $\mathbf{R} \in \Re^{n\times m}$ are positive semi-definite and definite matrices, respectively. Notice the values of matrices $\mathbf{Q}$ and $\mathbf{R}$ are set by the user and they have a major influence on the behaviour of the controller. In this work, $\mathbf{Q}$ and $\mathbf{R}$ are diagonal matrices. The calculation of the optimal gain $\mathbf{K}_{FB}$ is done by solving the state-dependent form of the algebraic Riccati equation.

The motorcycle controller structure is very similar to the one presented by [1] and implemented by [9]. This work focuses more on [9] as it treats the controller model to reflect the motorcycle dynamics.

The controller input variables are: the time t, the position vector $\mathbf{q}$ and the velocity vector $\dot{\mathbf{q}}$ of body 3 (Frame + Pilot), and a $flag$ value. For the output variables: the position δ, velocity $\dot{\delta}$ and acceleration $\ddot{\delta}$ of the steering angle. The controller algorithm is divided into two phases. The initialization ($flag = 2$), which happens at the beginning for $t = 0$, the steering angle and its time derivative are initialize. In the second phase, for every time step ($flag = 1$) during the motorcycle motion, it returns the steering angle, its velocity and acceleration.

Equation 20 computes the roll angle ϕ_M, where is used the entry of the transformation matrix $\mathbf{A}_3(3,2)$ corresponding to the rigid body $i = 3$ (Frame + Pilot).

$$\phi_M = \arccos(-\mathbf{A}_3(3,2)) - \frac{\pi}{2} \tag{20}$$

As known, the LQR control tries to minimize a cost function, leading to the variables of the state vector become as small as possible. Attending to this, the roll angle ϕ of the state vector $\mathbf{z}$, is given by the difference of the actual roll angle ϕ_M and a desired roll angle ϕ_{des}.

$$\phi = \phi_M - \phi_{des} \tag{21}$$

6.3. Prescribe a Trajectory
Curving in a constant radius curve is the simpler scenario to demonstrate the capability of the motorcycle controller. Starting at $v = 20m/s$, it was defined a desired roll angle of $\phi_{des} = 0.5[rad]$ at $t = 0.6[s]$, where at this time the motorcycle is practically stable. Figure 12 shows some of the time steps taken from SAGA software in the curve scenario.

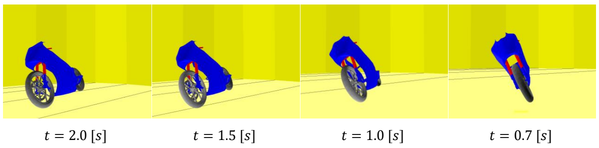

Figure 12: Time steps in curve scenario.

In order to accomplish this curving scenario, some modification were made. As identified by [9], the entry $\mathbf{C}(4,1)$ of the matrix $\mathbf{C}$ is responsible for the steering angle's interaction with the leaning angle. To achieve better results, this entry was set to $\mathbf{C}(4,1) = -80$. Modifications to the weighting matrix $\mathbf{Q}$ were necessary, leading to more weight to the steering position. $\mathbf{Q}_{diag} = \begin{bmatrix}100 & 1 & 1 & 1\end{bmatrix}$ and $\mathbf{R} = \begin{bmatrix}1\end{bmatrix}$.

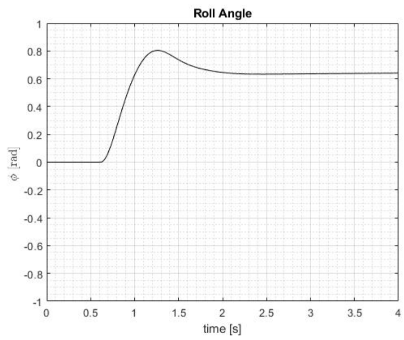

Figure 13: Roll angle ϕ_M over the time in curve scenario.

It can be observed a smooth transition until the stabilization of the roll angle, however exist overshoot. The final roll angle also presents an error, possible derived from coefficient $\mathbf{C}(4,1)$. It was observed, when the coefficient approaches 0, the error in the final roll angle gets very small but the overshoot increases significantly, leading sometimes to an instability. When the coefficient becomes more negative, the opposite happens. In initial simulations, it was verified an oscillation of the steering. To resolve that, the steering damper coefficient was set to $C_\delta = 20[Nms/rad]$.

Curve counter curve, or curve in S shape, raise other challenges for the motorcycle controller. In this scenario, the motorcycle change the roll angle from $\phi_{des} = 0.5[rad]$ to $\phi_{des} = -0.5[rad]$ almost in an instant. Also starting with $v = 20[m/s]$, it was defined a roll angle $\phi_{des} = 0.5[rad]$ at $t = 0.6[s]$ and a desired roll angle $\phi_{des} = -0.5[rad]$ at $t = 3.5[s]$. Also for this scenario, the values of $\mathbf{C}(4,1) = -80$ was maintained as well as the values of the matrices $\mathbf{Q}$ and $\mathbf{R}$. The steering damper coefficient $C_\delta = 20[Nms/rad]$ also remains unchanged.

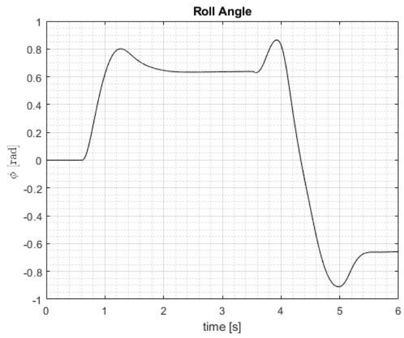

Figure 14: Roll angle ϕ_M over the time in curve counter curve scenario.

In the transition of roll angle values at $t = 3.5[s]$, as expected, the overshoot value is more salient. The error of the roll angle is the same, even to the left side, after the stabilization of the motorcycle.

7. Conclusions and Future Work

The concept of a semi-empirical tire model reveals the necessity of a great amount of tire parameters database, making it very accurate when applied to the correct tire geometry. Unfortunately, in the literature, it was not possible to find the tire database for the tires used, leading to compute less realist forces and moment applied on the tires. Although, an easy and versatile implementation of the *Magic Formula* tire model is described. The next objective of this work was the construction of the motorcycle multibody model of TLM03e prototype, allowing future studies of the prototype's dynamic aspects in more detail.

Finally, the motorcycle dynamic behaviour was evaluated under the conditions of the controller. A simple reduced model is chosen to control the motorcycle over different scenarios. Even though the simplified equations include a tire model, this is not consistent with the Pacejka tire model used in the motorcycle model. This difference between tire models, along with the imprecise tire model allocation on the motorcycle model, may reflect in the result of the roll angle achieved in the curve scenarios. As stated in Chapter 6, the change of the coefficient $\mathbf{C}(4,1)$ is fundamental to motorcycle stability. A major negative value of the coefficient results in less overshoot, but a greater error in the roll angle. If the coefficient becomes close to zero, stability problems can be found mainly for larger roll angles. The vehicle motion is too sensitive to the coefficients prescribed for the matrices $\mathbf{Q}$, $\mathbf{R}$ and $\mathbf{C}$. A more reasonable selection of these coefficients is still an open question that needs to be addressed.

The velocity profile of the motorcycle along the track is a quantity that needs to be tracked in order to achieved a least time lap. The controller must be be further developed to enforce that selected velocity profile, along the track, be achieved. The idea of achieving a minimal time lap involves not only an optimal trajectory, with its corresponding optimal velocity profile, but also the tuning of the motorcycle setup, which optimization methods are promising tools.

Acknowledgements
I begin by expressing my gratitude to my supervisor, Professor Jorge Ambrósio, for all his commitment and availability throughout the completion of this work. His enthusiasm and support were essential to stay focused and achieve the necessary motivation. To all my colleagues in the TLMoto team, for all the experiences and knowledge shared over the last few years. With them, my taste for motorcycling intensified.

References

[1] P. Antos and J. A. C. Ambrósio. A Control Strategy for Vehicle Trajectory Tracking Using Multibody Models. *Multibody System Dynamics*, 11(4):365–394, 5 2004.

[2] J. Baumgarte. Stabilization of constraints and integrals of motion in dynamical systems. *Computer Methods in Applied Mechanics and Engineering*, 1(1):1–16, 1972.

[3] V. Cossalter. *Motorcycle Dynamics (Second Edition)*. 2006.

[4] T. K. Dao and C. K. Chen. Path tracking control of a motorcycle based on system identification. *IEEE Transactions on Vehicular Technology*, 60(7):2927–2935, 2011.

[5] G. Gilardi and I. Sharf. Literature survey of contact dynamics modelling. *Mechanism and Machine Theory*, 37(10):1213–1239, 2002.

[6] G. Gim and P. E. Nikravesh. Analytical model of pneumatic tyres for vehicle dynamic simulations. Part 1. Pure slips. *International Journal of Vehicle Design*, 11(6):589–618, 1990.

[7] G. Gim and P. E. Nikravesh. Analytical model of pneumatic tyres for vehicle dynamic simulations. Part 2. Comprehensive slips. *International Journal of Vehicle Design*, 12(1):19–39, 1991.

[8] G. Gim and P. E. Nikravesh. Analytical model of pneumatic tyres for vehicle dynamic simulations. Part 3. Validation against experimental data. *International Journal of Vehicle Design*, 12(2):217–228, 1991.

[9] K. Huyge. Multibody Motorcycle , modelling and control. page 75, 2005.

[10] W. Langson and A. Alleyne. Multivariable bilinear vehicle control using steering and individual wheel torques. *Journal of Dynamic Systems, Measurement and Control, Transactions of the ASME*, 121(4):631–637, 1999.

[11] Y. Marumo and M. Nagai. Steering control of motorcycles using steer-by-wire system. *User Modeling and User-Adapted Interaction*, 45(5):445–458, 2007.

[12] P. E. Nikravesh. Computer Aided Analysis Mechanical Systems. 1988.

[13] H. B. Pacejka. *Tyre and Vehicle Dynamics*. Elsevier, 2nd edition, 2006.

[14] R. Sharp. Stability, Control and Steering Responses of Motorcycles. *Vehicle System Dynamics*, 35:291–318, 2001.

[15] R. Sharp, S. Evangelou, and D. Limebeer. Advances in the Modelling of Motorcycle Dynamics. *Multibody System Dynamics*, 12:251–283, 2004.

[16] R. S. Sharp. The Stability And Control Of Motorcycles. *Vehicle System Dynamics*, 13(5):316–329, 1971.

[17] R. S. Sharp. Motorcycle steering control by road preview. *Journal of Dynamic Systems, Measurement and Control, Transactions of the ASME*, 129(4):373–381, 2007.

[18] Y. Shen, D. Xiang, X. Wang, L. Jiang, and Y. Wei. A contact force model considering constant external forces for impact analysis in multibody dynamics. *Multibody System Dynamics*, 44(4):397–419, 2018.

[19] Tony Foale. *Motorcycle Handling and Chassis Design*. 2002.